Journal of Applied Polymer Science

Gasoline Permeation Behavior and Mechanical Properties of Polyamide 6/Nanoclay, Polyamide 6/PE-*g*-Maleic Anhydride Blend, and Polyamide 6/PE-*g*-Maleic Anhydride/Clay Nanocomposite

Ahmadreza Rouhollahi, Saied Nouri Khorasani, Alireza Farzadfar, Shahla Khalili, Mohammad Asgari
Department of Chemical Engineering, Isfahan University of Technology, Isfahan 84156-83111, Iran
Correspondence to: S. N. Khorasani (E-mail: saied@cc.iut.ac.ir)

ABSTRACT: In this article, polyamide 6 (PA6)/clay nanocomposites, PA6/polyethylene grafted maleic anhydride (PE-*g*-MA) blends, and PA6/PE-*g*-MA/clay nanocomposites were prepared and their gasoline permeation behavior and some mechanical properties were investigated. In PA6/clay nanocomposites, cloisite 30B was used as nanoparticles, with weight percentages of 1, 3, and 5. The blends of PA6/PE-*g*-MA were prepared with PE-*g*-MA weight percents of 10, 20, and 30. All samples were prepared via melt mixing technique using a twin screw extruder. The results showed that the lowest gasoline permeation occurred when using 3 wt % of nanoclay in PA6/clay nanocomposites, and 10 wt % of PE-*g*-MA in PA6/PE-*g*-MA blends. Therefore, a sample of PA6/PE-*g*-MA/clay nanocomposite containing 3 wt % of nanoclay and 10 wt % of PE-*g*-MA was prepared and its gasoline permeation behavior was investigated. The results showed that the permeation amount of PA6/PE-*g*-MA/nanoclay was 0.41 g m^{-2} day^{-1}, while this value was 0.46 g m^{-2} day^{-1} for both of PA6/3wt % clay nanocomposite and PA6/10 wt % PE-*g*-MA blend. © 2013 Wiley Periodicals, Inc. J. Appl. Polym. Sci. **2014**, *131*, 40150.

KEYWORDS: polyamides; nanostructured polymers; clay; mechanical properties; blends

Received 10 June 2013; accepted 2 November 2013
DOI: 10.1002/app.40150

INTRODUCTION

Polymeric materials used as gasoline conveyor in automobile industry for applications such as fuel tubes must have barrier properties against gasoline permeation. Interesting permeation characteristics have been obtained by blending polar polymer matrices with organo-modified clays. In the nanocomposites, the polymer matrix is the permeable phase, while the dispersed nanolayers form the barrier phase. The enhancement in barrier properties of a nanocomposite is as a result of expected reduced solubility which is due to reduction in volume of the polymer matrix. It could also be due to the formation of exfoliated morphology resulting enhancement in the tortuous path for molecular diffusion in presence of high aspect ratio nanoclays throughout the matrix, as presented in Figure 1.[1,2]

Among polar polymers which have barrier properties against gasoline, polyamide 6 (PA6) has been under a lot of attention. Having low permeation against gasoline due to its polar structure, PA6 also has satisfactory mechanical properties. Yet, researchers in this area have tried to improve barrier properties of PA6.[3–10]

Gasoline consists of several materials like hydrocarbons, methanol, ethanol etc. The specific amount of each component is specified in standards such as ASTM D471. As polyamide could be swollen against alcoholic chemicals in gasoline by absorption of those substances, blending PA6 with modified polyethylene (PE) such as PE grafted maleic anhydride (PE-*g*-MA) could be applied. PE-*g*-MA has barrier properties against those chemicals and so as to enhance the permeation properties of PA6. Besides, anhydride groups of PE-*g*-MA could react with PA6 amine chain end groups, thus the absorption of alcoholic chemicals by PA6, and therefore it's swelling against gasoline will be reduced. Besides, the phase separation and also coalescence phenomenon will be prevented in PA6/PE-*g*-MA blend due to chemical interaction that could occur between PA6 and PE-*g*-MA in comparison with PA6/PE blends.[3,11]

Studying on decreasing the amount of permeation of polar materials such as water from PA6 has led to several approaches like applying nanocomposites, blending PA6 with polyolefins, or combination of these two methods.[4–7]

The barrier properties of PA6 against gases,[8,9] methanol[10,12,13] and other solvents were investigated by some other researches.[10] In addition, some researchers investigated the permeation properties of multi-layer PA6 nanocomposites as fuel tubes.[14–16] Fornes et al. investigated the effect of different nanoclays on

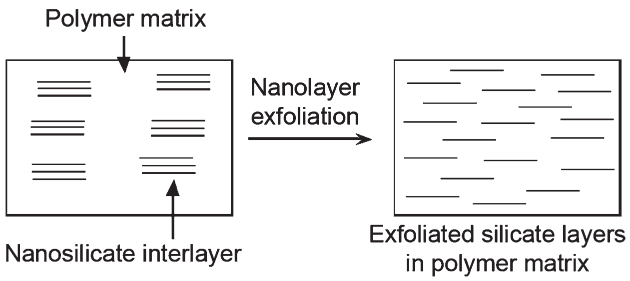

Figure 1. Schematic representation of nanolayer exfoliations in the bulk of polymer matrix.

morphology and mechanical properties of PA6 nanocomposites. They reported that three factors: (i) a long alkyl chain on ammonium ion, (ii) methyl groups instead of 2-hydroxyl ethyl groups, and (iii) an appropriate amount of active amine in nanoclay lead to a better exfoliation, higher hardness and an increase in tensile strength of PA6 nanocomposites. Among different applied nanoclays, cloisite 30B showed the best exfoliation in nanocomposite samples.[17,18] Brule et al. investigated the permeation of oxygen and styrene in PA6/polyolefin/compatibilizer/nanoclay nanocomposites. The results showed that styrene was embedded in the polyolefin and the polyolefin part was swollen. The polyolefin also had a barrier role for oxygen.[9] Low et al. have prepared PA6/nanoclay nanocomposite films to investigate humidity absorption in PA6. They showed that in the nanocomposite samples the permeation coefficient decreased by addition of nanoclay.[4] Similarly, other researchers have reported the same results for PA6 nanocomposites.[5–7] Yeh et al. investigated the effects of annealing on gasoline permeation properties of PA6/PE and PA6/PE/Acrylic acid blends. Among all of the prepared samples, PA6 has the highest barrier properties and neat PE has the lowest gasoline permeation properties. Moreover, in annealed samples, the barrier properties decreased with increasing the time and temperature of annealing.[19–21] Moghri et al. investigated some rheological and morphological properties of PA6 nanocomposites. The results showed that exfoliation was completely occurred when using 3 and 5 wt % of nanoclay, but the complete exfoliation did not occur by using 7 wt % of nanoclay. To measure the gasoline permeation properties of nanocomposites, gasoline weight loss method were used according to ASTM D2684. The results showed that the permeation of gasoline from samples was decreased with respect to neat PA6 and the lowest permeation belonged to sample containing 5 wt % of nanoclay.[22]

The allowable gasoline permeation from fuel tubes has been set at 2 g m^{-2} day^{-1} by the Institute of Petroleum Performance Specification (IPPS). However, in some countries, the acceptable permeation of gasoline is up to 4 g m^{-2} day^{-1}.[3]

In this research, first nanocomposites of PA6/nanoclay and blends of PA6/PE-*g*-MA were prepared and their barrier properties against gasoline and some mechanical and morphological properties were investigated. After that, according to the optimum fuel permeation results obtained from the PA6/nanoclay nanocomposites and PA6/PE-*g*-MA blends, a combination of these two methods was applied to see the synergistic influences of nanocomposites and blending in lowering the gasoline permeation. For this, nanocomposite of PA6/PE-*g*-MA/nanoclay was prepared and their permeation behavior and some of their mechanical properties were investigated.

EXPERIMENTAL

Materials

PA6 (Akulun F136 C1) was from DSM, Netherland. PE-*g*-MA was obtained from Kimia Javid, Iran, under the name of Kimcross 1122 (MFI of 1 g/10 min according to ISO1133) with one percent of grafting. Modified nanoclay (Cloisite 30B), alkyl quaternary ammonium salt bentonite, with basal spacing (d_{001}) of 1.85 nm, moisture percent < 3%, density of 98 g/cc, and average dry particle size of less than 10 μm was supplied by Southern Clay Products.

Samples Preparation

All of the raw materials (PA6, PE-*g*-MA, and nanoclay) were dried at 80°C for 16 h in a vacuum oven.

Then they were mixed physically at dry conditions with diverse weight percents as presented in Table I.

The mixtures were melt blended using a co-rotating twin screw extruder (SH-20 model, Nanjing Giant, China), L/D = 40 at screw speed of 400 rpm. The extruder has two high-quality mixing zones with kneading parts to enhance the dispersion and distribution mixing of the nanoclays in PA6 matrix. It also consists of six heating zones with the temperature of 130°C, 150°C, 180°C, 220°C, 230°C, and 240°C by each zone. The extrudate were pelletized. Then the pelletized mixtures were injection molded.

Attenuated Total Reflectance-Infra Red (ATR-IR)

To investigate the reaction occurred between amine end groups of PA6 chain and anhydride groups of PE-*g*-MA, the ATR-IR (Shimadzu model Prestige-21, Japan) test was applied. The wave length range was 400–4000 cm^{-1}. To prepare the specimens for this test, the samples of PA6 and PE-*g*-MA separately, and blend of PA6/30 wt % PE-*g*-MA was placed in an oven at 80°C for 20 h to remove their moisture. Then the films with dimensions of 48 × 12.5 × 1 mm^3 were prepared by hot press technique.

Table I. Constituent Weight Percents in Formulation of PA6/Nanoclay Nanocomposite, PA6/PE-*g*-MA[a] Blend, and PA6/PE-*g*-MA/Nanoclay Nanocomposite Samples

Sample code	PA6	Nanoclay	PE-*g*-MA
1	100	–	–
2	99	1	–
3	97	3	–
4	95	5	–
5	90	–	10
6	80	–	20
7	70	–	30
8	87	3	10

[a] Polyethylene-*g*-maleic anhydride.

Scanning Electron Microscopy (SEM)

The morphology of the specimens and also the phase morphology in PA6/PE-*g*-MA blend were investigated using a SEM technique (Philips XL300 model microscope, Netherland).

X-ray Diffraction (XRD) Test

XRD test is a technique to determine the phase structures and composition of a material. In X-ray method, parallel radiations of X-ray with the same energy are irradiated to the specimens, considering the fact that the irradiated X-ray wave length is an order of distance between atoms of the material. Here, the wave length is an order of the distance between the silicate nanolayers.

To analyze the structure of the nanocomposites, X-ray diffraction method (Brucker model D8Advance, Germany) was used. The results also were applied to investigate the type of placement of nanolayers and their exfoliation in the PA6 matrix. This method is very useful in determining the structure between nanolayers in the nanocomposites. The diffraction angle range (2θ) was 0.5–10°, by way of rotary scanning of 0.04 within 2 s. In this range, PA6 shows no peak, while nanosilicate shows one peak. The samples used for the XRD test were films with dimensions of 3 × 3 mm^2, which were produced by hot press technique.

Ash Test

Ash test (Reometric scientifitic TGA) was used to measure the amount of nanoclay in nanocomposite samples. For this, the PA6 nanocomposite samples are weighted first which are considered as W_1. Then the samples are placed in a furnace at 900°C for 45 min. According to the nanoclay datasheet, nanoclays must show 30% weight loss, which leaves 70% of nanoclays at these conditions. PA6 is completely destroyed at this temperature. After that, the crucible containing the sample is weighted. This weight minus the crucible itself is considered as W_2. The ash percent and the real amount of nanoclay in the samples are calculated based on eqs. (1) and (2).

$$\%Ash=\frac{W_2}{W_1}\times 100 \tag{1}$$

$$\%Nanoclay=\frac{\%Ash}{0.7} \tag{2}$$

where the W_1 is the nanocomposite sample weight before burning and W_2 the weight of the ash remained after burning of the sample.

Gasoline Permeation Behavior

The permeation test was carried out according to ASTM D2684. Therefore, the samples were injected to the form of lids with 50-mm diameter and 1.9-mm thickness. Then the lids were subjected and fitted on a glass beaker. To seal the samples, a type of epoxy glue (epoxy steel adhesive which is anti gasoline, anti freeze, and resistant to the most of solvents and it includes two parts of the epoxy resin and polyamine hardener, produced by Eagiestar manufacturer) was applied. The beakers were maintained at 23°C and the weight loss of each container measured every day. The gasoline used for this study is lead free gasoline form the refinery of Isfahan, Iran.

Tensile and Impact Properties

The tensile behavior of the specimens was determined using a Zwick/Roell tensile tester (model Z020) according to ISO 527 at room temperature, with specimen cross section of 40 mm^2. The test speed was 50 mm/min. The impact strength was evaluated based on ISO 179, using a Zwick/Roell impact tester (model HIT5.5P) with 4J pendulum. The specimen dimensions for the impact test were 50 × 12 × 3 mm^3. Charpy impact specimens were injection moulded. The notch depth was 1 mm with the angle of 45°.

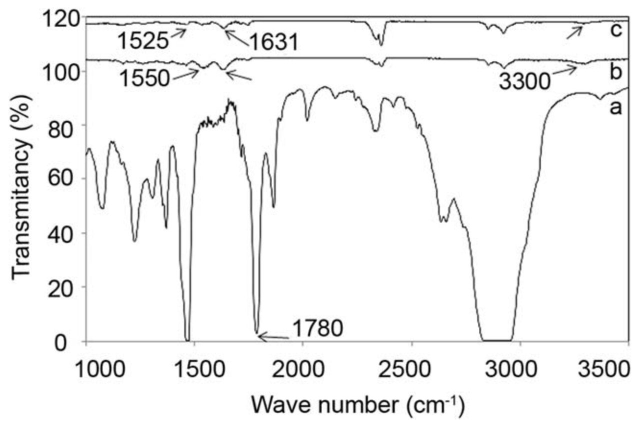

Figure 2. ATR-IR spectra of (a) PA6, (b) PE-*g*-MA, and (c) PA6/30 wt % PE-*g*-MA blend.

RESULTS AND DISCUSSION

ATR-IR Results

FTIR analysis is a technique usually applied to study the maleation reaction. To investigate the bond formation between amine end groups in PA6 and anhydride group in PE-*g*-MA which leads to formation of imides groups in PA6/PE-*g*-MA blend,[11] ATR-IR technique was applied. The ATR-IR spectra of pure PA6, PE-*g*-MA, and PA6/PE-*g*-MA blend are shown in Figure 2(a–c), respectively. According to Figure 2(c), the peaks in wavelengths of 3260, 1631, and 1525 cm^{-1} are related to the N—H bond stretch, asymmetric C═O stretch, and N-H bending, respectively, which indicates the bond formation between amine group in PA6 and anhydride group of PE-*g*-MA according to the researchers in this area. These results are consistent with the research work of Chaui et al.[23] and Iqbal et al.[24]

SEM Results of PA6/PE-g-MA

SEM micrographs of tensile fracture surfaces of pure PA6 and PA6/PE-*g*-MA blends are presented in Figure 3. As it can be seen from the figure, there are continuous surfaces for PA6, PA6/10 wt % PE-*g*-MA, and PA6/30 wt % PE-*g*-MA in Figure 3(a,b,d), however, the SEM micrograph of PA6/20 wt % PE-*g*-MA shows a rough surface as shown in Figure 3(c). This could be due to the fact that by increasing the amount of PE-*g*-MA in PA6/PE-*g*-MA blends, the phase inversion could occur as PE-*g*-MA has lower viscosity in comparison with PA6, which lets the PE-*g*-MA be the matrix and PA6 be the disperse phase. The rough surface in SEM of PA6/20 wt % PE-*g*-MA is probably due to phase separation between PA6 matrix and PE-*g*-MA disperse phase in this blend.[24–26]

XRD Test Results

XRD test is a method to study the dispersion of nanoclay layers in polymer matrix. As it is shown in XRD graph of pure

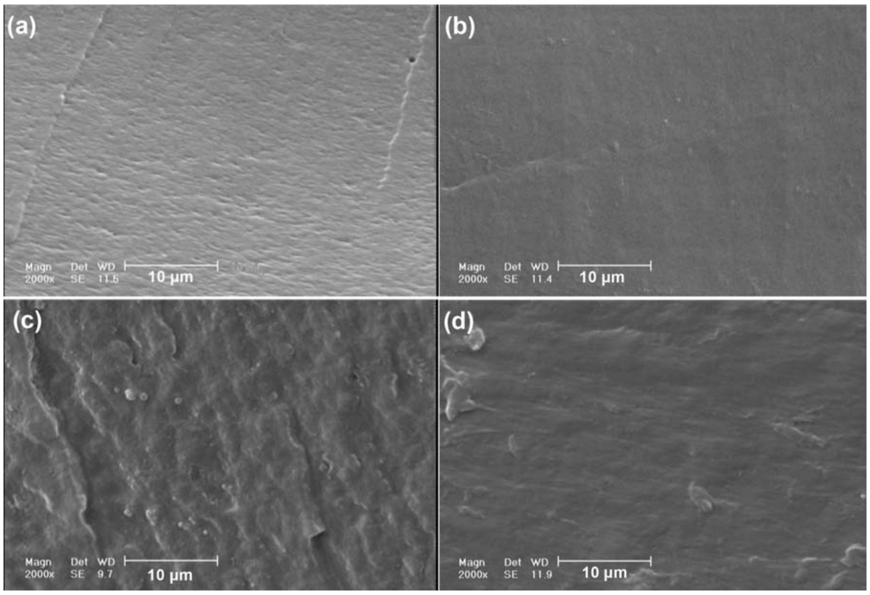

Figure 3. SEM photographs of tensile fracture surfaces of (a) Pure PA6, (b) PA6/10 wt % PE-*g*-MA, (c) PA6/20 wt % PE-*g*-MA, and (d) PA6/30 wt % PE-*g*-MA.

nanoclay in Figure 4(a), for pure nanoclay a peak was appeared in $2\theta = 4.8°$ that it is because of regular direct distance between layers of nanoclay layers. Besides, there is no peak in XRD pattern of pure PA6 sample as it was revealed in Figure 4(b). In Figure 4(c–e), which belong to the XRD graphs of 1 wt %, 3 wt %, and 5wt % nanoclay nanocomposites, respectively, it can be seen that by mixing nanoclay with PA6 during melt blending, the peak of nanoclay has been disappeared. This is due to the good exfoliation and dispersion of nanoclay layers in PA6 matrix, as it was also explained by Paci et al.[27]

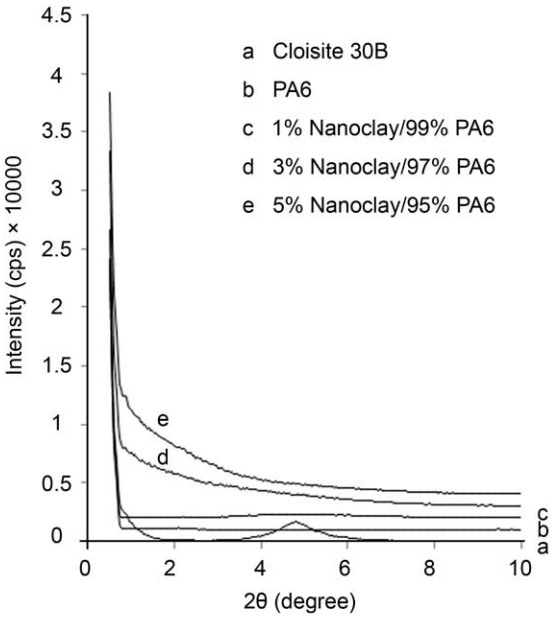

Figure 4. XRD curves of (a) Cloisite 30B, (b) PA6, (c) PA6/1 wt % nanoclay, (d) PA6/3 wt % nanoclay, and PA6/5 wt % nanoclay nanocomposite.

Ash Test Results

The results showed that 30 wt % of nanoclay were deteriorated at 900°C and therefore 70 wt % of the nanoparticles remained, which is in accordance with the Cloisite 30B datasheet. For this, the ash content in nanocomposite samples with 1, 3, and 5 wt % of nanoclay were 0.67, 2.0, and 3.32 wt %, respectively. Since, nanoclay has weight loss by 30%, the initial amount of nanoclay in nanocomposites containing 1, 3, and 5 wt % of nanoclay obtained 0.95, 2.86, and 4.75 wt %, respectively, based on eqs. (1) and (2).

Gasoline Permeation Results

The permeation results obtained for PA6/nanoclay nanocomposites and PA6/PE-*g*-MA blends are presented in Figure 5. According to the figure, the sample with 3 wt % of nanoclay had the lowest gasoline permeation among the nanocomposite samples. By enhancing the nanoclay content from 3wt % to 5 wt % in PA6/clay nanocomposite, the permeation increases. It could be due to reason that by increasing the amount of clay, the distance increment of nanoclay plates becomes more difficult. Among the blend samples, the sample with 10 wt % of PE-*g*-MA showed the lowest gasoline permeation. Therefore, a sample containing 3 wt % of nanoclay and 10 wt % of PE-*g*-MA was prepared and its gasoline permeation behavior was investigated. The results showed that the permeation amount of PA6/PE-*g*-MA/nanoclay nanocomposite was 0.41 g m^{-2} day^{-1} while this value was 0.46 g m^{-2} day^{-1} for 3 wt % of nanoclay nanocomposite and PA6/10 wt % PE-*g*-MA blend. This observation could also be as a result and also support of the intercalation/exfoliation of silicate nanolayers in the bulk of polymer matrix, as exfoliation of nanolayers plays an important role on permeation properties.

Tensile and Impact Test Results

The results of tensile and impact strength are shown in Table II. As it is clear from the table, the elastic modulus and tensile

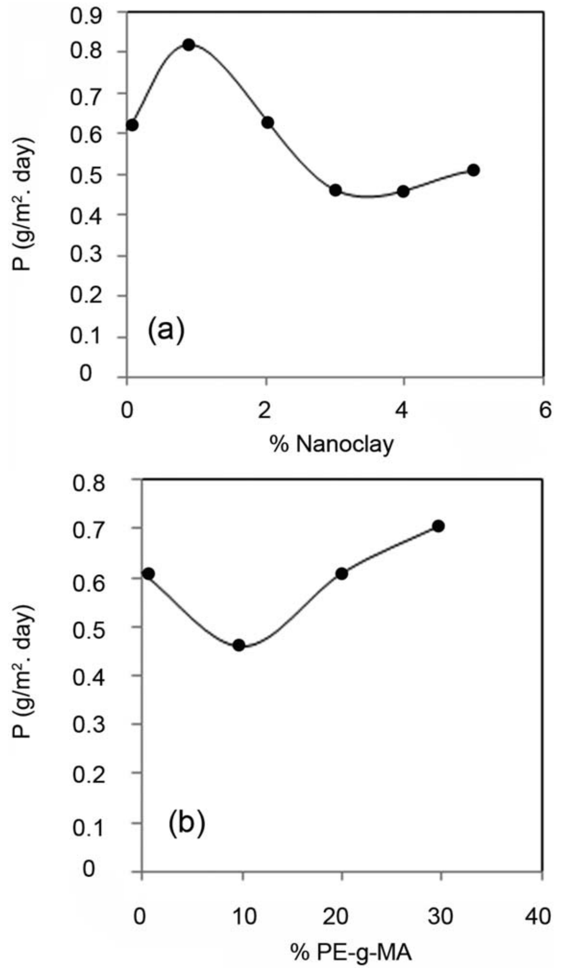

Figure 5. Permeation of (a) PA6/nanoclay nanocomposites versus nanoclay wt % and (b) PA6/PE-*g*-MA versus PE-*g*-MA wt %.

strength of PA6 nanocomposite samples increased from 18% to 45% and 12% to 47%, respectively with increasing the amount of nanoclay. This is due to higher elastic modulus and reinforcing effects of silicate nanolayers, respectively. It can be seen that the strength of PA6/5wt % nanoclay composite is greater than that of PA6/3wt % nanocomposite sample, which is due to reinforcing effect and higher mechanical properties of nanosilicate layers in the bulk of the PA6 matrix. The enhancement in tensile strength of PA6/nanoclay nanocomposites could also support the exfoliation of nanoclay layers in the bulk of the matrix, which leads to higher surface area of nanolayers, causing more attraction with PA6 matrix and therefore, leading to higher tensile strength of PA6/nanoclay nanocomposites. This observation was also supported by XRD test results. Nonetheless, elongation at break was decreased with increasing the amount of nanoclay. In PA6 blend samples, the elastic modulus and tensile strength decreased from 7% to 31% and 14% to 42%, respectively with increasing the amount of PE-*g*-MA from 10 to 30 wt %, but elongation at break increased with increasing the amount of PE-*g*-MA from 10% to 30%, which is due to higher elongation at break of PE-*g*-MA in comparison with PA6. In PA6/PE-*g*-MA/nanoclay nanocomposite, the elastic modulus and elongation at break increased and tensile strength decreased comparing with that for pure PA6. Furthermore, the results of impact test showed that the impact strength of nanocomposites decreased from 35% to 47% with increasing the amount of nanoclay from 1% to 5% in nanocomposites in comparison with that of pure PA6, however, in PA6/PE-*g*-MA blends, the impact strength of samples increased from 455% to 1344% with increasing the amount of PE-*g*-MA from 10% to 30% comparing with impact strength of PA6, which is due to higher toughness of PE-*g*-MA compared with PA6. Furthermore, the impact strength of PA6/PE-*g*-MA/nanoclay nanocomposite sample increased with respect to that for pure PA6.

CONCLUSION

As the XRD test results showed, exfoliation in nanocomposite samples with 3 and 5 wt % of nanoclay occurred. The SEM micrographs showed continuity in PA6/PE-*g*-MA blends. However, phase separation might have occurred in PA6/20wt % PE-*g*-MA blend due to flake like fracture surface. ATR-IR spectra confirmed the reaction occurred between amide groups in PA6 and maleic anhydride grafted on PE-*g*-MA. The gasoline permeation test results showed that the sample with 3 wt % of nanoclay had the lowest gasoline permeation among nanocomposite samples and also the sample with 10 wt % of PE-*g*-MA revealed the lowest gasoline permeation among blend samples. In addition, the final PA6/PE-*g*-MA/nanoclay nanocomposite sample

Table II. Mechanical Properties of PA6/Clay Nanocomposite, PA6/PE-*g*-MA[a] Blend, and PA6/PE-*g*-MA/Clay Nanocomposite Samples

Sample code	Elastic modulus (MPa)	Tensile strength (MPa)	Elongation at break (%)	Notched Charpy impact strength (kJ/m^2)
1	2310	77.7	25	6.98
2	2720	87	17	4.54
3	3030	92.5	12	4.36
4	3350	96.2	17	3.71
5	2150	66.7	21	38.72
6	1850	54.3	150	75.53
7	1590	45.3	160	100.81
8	2510	69.5	49	13.73

[a] Polyethylene-*g*-maleic anhydride.

had the lowest gasoline permeation among all samples which indicates the synergic effect of combination of nanocomposite with blending technique. The results of tensile tests showed that the elastic modulus and tensile strength increased and elongation at break decreased with increasing the amount of nanoclay in nanocomposites. Moreover, the elastic modulus and tensile strength decreased and elongation at break increased with increasing the amount of PE-*g*-MA in blend samples. Also, in PA6/PE-*g*-MA/nanoclay nanocomposite, the elastic modulus and elongation at break increased and the tensile strength decreased with respect to pure PA6. The impact test results showed that the impact strength of nanocomposites decreased with increasing the amount of nanoclay, while in blend samples the impact strength increased with increasing the amount of PE-*g*-MA.

ACKNOWLEDGMENTS

The authors thank the R&D manager of Kimia Javid Co., Isfahan Iran, for their corporation in this research.

REFERENCES

1. Choudalakis, G.; Gotsis, A. *Eur. Polym. J.* **2009**, *45*, 967.
2. Paul, D.; Robeson, L. *Polymer.* **2008** *49*, 3187.
3. Greenwood, J. H. *Polym. Test.* **2001**, *20*, 383.
4. Low, H.; Liu, T.; Loh, W. *Polym. Int.* **2004**, *53*, 1973.
5. Picard, E.; Gérard, J. F.; Espuche, E. *J. Membr. Sci.* **2008**, *313*, 284.
6. Abacha, N.; Kubouchi, M.; Sakai, T. *Exp. Polym. Lett.* **2009**, *3*, 245.
7. Li, Q.; Wei, Q.; Wu, N.; Cai, Y.; Gao, W. *J. Appl. Polym. Sci.* **2008**, *107*, 3535.
8. Picard, E.; Vermogen, A.; Gérard, J. F.; Espuche, E. *J. Membr. Sci.* **2007**, *292*, 133.
9. Brulé, B.; Flat J. J. Wiley Online Library, **2006**; p 210.
10. Jiang, T.; Wang, Y.; Yeh, J.; Fan, Z. *Eur. Polym. J.* **2005**, *41*, 459.
11. Jiang, C.; Filippi, S.; Magagnini, P. *Polymer.* **2003**, *44*, 2411.
12. Zhang, Y.; Yang, J.; Ellis, T.; Shi, J. *J. Appl. Polym. Sci.* **2006**, *100*, 4782.
13. Tamura, K.; Uno, H.; Yamada, H.; Umeyama, K. *J. Polym. Sci. Polym. Phys.* **2009**, *47*, 583.
14. Kerschbaumer, F. US Pat. 5219003, **1993**.
15. Siour, D.; Denizart, O.; Echalier, B. US Pat. 6177162, **2001**.
16. Merziger, J. US Pat. 6302153, **2001**.
17. Fornes, T.; Yoon, P.; Keskkula, H.; Paul, D. *Polymer* **2001**, *42*, 9929.
18. Fornes, T.; Yoon, P.; Hunter, D.; Keskkula, H.; Paul, D. *Polymer* **2002**, *43*, 5915.
19. Yeh, J. T.; Chang, S. S.; Yao, H. T.; Chen, K. N.; Jou, W. S. *J. Mater. Sci.* **2000**, *35*, 1321.
20. Yeh, J. T.; Chen, C. H.; Shyu, W. D. *J. Appl. Polym. Sci.* **2001**, *81*, 2827.
21. Yeh, J. T.; Huang, S. S.; Yao, W. H. *Macromol. Mater. Eng.* **2002**, *287*, 532.
22. Moghri, M.; Garmabi, H.; Molajavadi, V. *J. Vinyl. Addit. Techn.* **2010**, *16*, 195.
23. Chuai, C.; Iqbal, M.; Tian, S. *J. Polym. Sci. Polym. Phys.* **2010**, *48*, 267.
24. Iqbal, M.; Chuai, C.; Huang,Y.; Che, C. *J. Appl. Polym. Sci.* **2010**, *116*, 1558.
25. Favis, B. *Polymer* **1994**, *35*, 1552.
26. Utracki, L. Polymer Blends; Smithers Rapra Publishing: Ohio, **2000**; Vol. *11*.
27. Paci, M.; Filippi, S.; Magagnini, P. *Eur. Polym. J.* **2010**, *46*, 838.